Journal of Hydrology 534 (2016) 31–41

Contents lists available at ScienceDirect

Journal of Hydrology

journal homepage: www.elsevier.com/locate/jhydrol

Vertical profile of rain: Ka band radar observations at tropical locations

Saurabh Das [1], Animesh Maitra *

Institute of Radio Physics and Electronics, University of Calcutta, 92, Acharya Prafulla Chandra Road, Kolkata 700009, India

ARTICLE INFO

Article history:
Received 1 April 2014
Received in revised form 23 December 2015
Accepted 26 December 2015
Available online 4 January 2016
This manuscript was handled
by A. Bardossy, Editor-in-Chief,
with the assistance of Harald Kunstmann,
Associate Editor

Keywords:
Vertical profile of reflectivity
Radar
Drop size distribution
Tropical rain
Ka band

SUMMARY

Information of vertical rain structure is important for accurate quantitative precipitation estimation from weather radars and space-borne radars. In this paper, some characteristics of the vertical rain structure observed using a Ka band Micro Rain Radar at three tropical locations in India are presented. The average vertical structure is studied in terms of drop size distribution (DSD), fall velocity, rain rate, liquid water content and radar reflectivity profile. The changes in vertical rain structure with rain rate is observed to be significant only above 20 mm/h in Ahmedabad and Trivandrum, although, in Shillong, significant variation is observed starting from 2 mm/h. Results show a significant negative slope of the fall velocity of rain drops and Ka band radar reflectivity up to melting layer height for rain rate above 20 mm/h indicating a shift in the drop size distribution (DSD) toward lower size at all sites. The near ground measurements show strong variation of rain structure for all rain rates. The mean DSD near ground (<1 km) indicates the dominance of smaller drops during rain rates below 2 mm/h, but significant increase in drop size in rain rate above 20 mm/h. The findings suggest using different retrieval techniques for near ground rain estimation than the rest of the height profile as well for high rain rate events.

1. Introduction

Radar provides a unique tool to measure the precipitation with a large aerial coverage. However, the space borne-radars as well ground based weather radars do not always represent the surface rain characteristic accurately (Peters et al., 2005; Thurai et al., 2003; Kirstetter et al., 2013). The major source of this inaccuracy is due to vertical variation of radar reflectivity, especially near the melting layer. The bias in the vertical profile of reflectivity (VPR) also arises due to the assumptions of constant reflectivity up to melting layer height from the surface. The evolution of rain drops via melting, coalescence, break up and evaporation are primarily responsible for this variation of VPR. The change in drop size distribution (DSD) along the vertical direction may have a significant effect in the estimated rain rate profile. Studies using radars have been performed in the past to address this issue, notably in relation to the Tropical Rainfall Measuring Mission (TRMM) (Peters et al., 2005; Thurai et al., 2003; Cluckie et al., 2000). However, due to lack of experimental measurements of actual VPR, most studies concentrated on adjusting bias in the ground precipitation estimation of radar data by using ground based instruments (Koistinen and Michelson, 2002; Bellon et al., 2007; Seo et al., 2000).

A very limited number of radar observations are reported which studied the variation of VPR in connection with the change in DSD spectrum over the height and how this variation influence the rain retrieval (Kirstetter et al., 2013; Cluckie et al., 2000). Peters et al. (2005) showed a significant shape transformation of DSD and Z-R relation from the ground to the melting layer for strong rain around the Baltic Sea in temperate regions. Strong variation of VPR in convective rain was also observed by Thurai et al. (2003) during radar campaign in Singapore in equatorial region. Similar observations are also reported by Das et al. (2010a,b) from Ahmedabad in tropical region. Zipser and Lutz (1994) reported contrasting features of VPR in mid-latitude and tropical continental locations with that of the tropical oceanic region. The seasonal variation of Z-R using ground based DSD measurements are also studied by various researchers (Rao et al., 2001; Kozu et al., 2006). Seasonal variations of vertical Z-R relation are also observed to be significant over Kolkata in tropical region (Das et al., 2011a,b). The characteristic difference of VPR between convective and stratiform rain was also reported by many researchers from these regions (Das et al., 2010a,b; Rudolph and Friedrich, 2013; Thurai et al., 2003).

* Corresponding author at: Institute of Radio Physics and Electronics, S.K. Mitra Centre for Research in Space Environment, University of Calcutta, 92, Acharya Prafulla Chandra Road, Kolkata 700009, India. Tel.: +91 33 2350 9116x28 (Office); fax: +91 33 2351 5828.

E-mail addresses: das.saurabh01@gmail.com (S. Das), animesh.maitra@gmail.com, am.rpe@caluniv.ac.in (A. Maitra).

[1] Presently at Center for Soft Computing Research, Indian Statistical Institute, 203 Barrackpore Trunk Road, Kolkata 700108, WB, India

http://dx.doi.org/10.1016/j.jhydrol.2015.12.053
0022-1694/

The previous results highlight significant vertical variation of the reflectivity profile during various phases of the precipitation (Bellon et al., 2005) as well as between different regions. The most significant variation is observed due to presence of melting layer in stratiform rain. The regions below the melting layer are assumed to be uniform. Most of the results suggest that the N_o adjustment technique (Thurai et al., 2003) is generally acceptable for rain rate estimation from radar data during stratiform precipitation below melting layer. However, for convective systems, these assumptions are no longer valid and multi-frequency measurements are suggested. The Global Precipitation Mission (GPM) satellite are having dual frequency radar in Ku and Ka band to improve the rain fall estimation from space.

In view of GPM satellite, further investigation on this topic is expected, especially from the regions where very limited or no information of VPR is available. In addition, rain observations in the Ka-band are also an important consideration due to heavy rain attenuation in this frequency band. Moreover, the variation of VPR near ground (<1 km) and above up to the melting layer is usually assumed to be similar which may need a closer examination since the instantaneous ground rain rate is more important for flood warning and other related early warning systems.

In this paper, we report some statistical observations of vertical rain structure obtained using a vertical looking Micro Rain Radar (MRR) in Ka band frequency at three tropical locations in India, namely, Trivundrum (8°29′N, 76°57′E), Ahmedabad (23°04′, 73°38′), and, Shillong (25°34′N, 91°53′E,), during 3 years (2006–2008) of the measurement period. The VPR and associated rain DSD are investigated for different rain rate regimes with a special emphasize on the lowest 1 km region to address these questions.

2. Instrument description and data

2.1. Site specifications

MRR data has been collected from three locations in the Indian region during the year 2006–2008. These three locations have different rain climatology. Trivundrum is situated in the southern peninsular region of India. Annual rainfall in this location is ~1800 mm and received rainfall during both south-west (SW) and north-east (NE) monsoon. According to Köppen–Geiger classification (Peel et al., 2007), Trivandrum has tropical wet and dry savanna climate. On the other hand, Ahmedabad is situated in the relatively dry location in western India with approximately

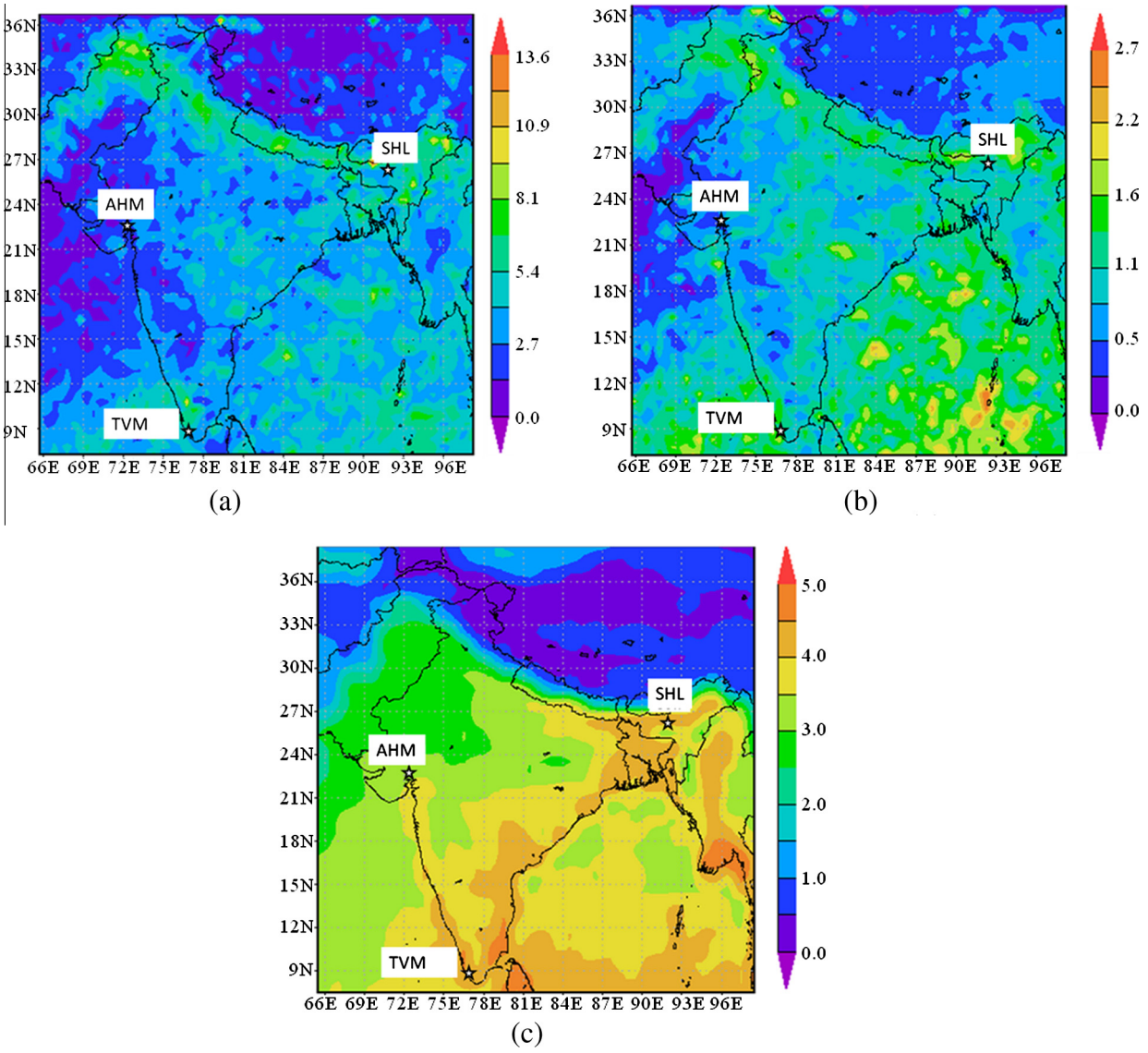

Fig. 1. Climatology of the experimental sites (a) average convective rain rates (mm/h), (b) average stratiform rain rates (mm/h) and (c) average water vapor (cm). Rain rate information is obtained from TRMM and water vapor data is obtained from AQUA-MODIS satellite.

Table 1
MRR specifications.

Frequency	24.1 GHz
Power	50 mW
Operation mode	FM-CW
Beam width	2°
Antenna type	Offset parabolic
Height resolution	200 m (minimum 10 m)
Temporal resolution	30 s (minimum 10 s)
Number of range gates	30
Spectral velocity resolution	0.191 m s^{-1}

800 mm annual rainfall. Rainfall in this location is mainly carried by the SW monsoon. Ahmedabad has a hot semi-arid climate. Shillong, which receives ~2400 mm annual rainfall, is a hilly mountainous region (~1.5 km above msl) on the Himalaya in northeastern India. Both SW and NE monsoon plays important role in the rain formation in this region. In addition, orographic rain due to the topography of this region is also important. It has a subtropical highland climate as per Köppen–Geiger classification.

Fig. 1 represents the climatic conditions of these locations for a typical year (2013). TRMM observed annual average convective and stratiform rain rates are shown in Fig 1(a) and (b) respectively. The average water vapor is also indicated in Fig. 1(c) as seen by MODIS instrument onboard AQUA satellite for the same year. It can be seen that the water vapor availability is high in both Shillong and Trivandrum than Ahmedabad throughout the year. The rain rate of both convective and stratiform type is highest in Shillong.

2.2. Micro rain radar

The Micro Rain Radar (MRR) is a Frequency Modulated Continuous Wave (FM-CW) Doppler radar at 24.1 GHz. This radar operates only in the zenith direction mode and, thus, can provide time series of various rain parameters measured using the Doppler principle. The specifications of MRR are given in Table 1. The retrieval of Doppler spectra and different rain parameters are well documented by many researchers (Atlas et al., 1973; Peters et al., 2005; Das et al., 2010a,b, 2011a,b). The basic principle is to measure the fall velocity of the falling rain drops and then using the Gunn and Kinzer (1949) relationship DSD is estimated. Once the DSD is estimated, other parameters can be calculated based on DSD.

MRR receives unavoidable noise with the echo signal at its input which must be estimated and removed before processing. MRR signal processing software includes a noise estimation module which assumed the noise signal as an Additive White Gaussian Noise (AWGN). The noise level is estimated by iteratively removing the spectral lines having power above the mean power of the spectrum until they are equal or less than the mean power. This final mean power is designated as the noise power and is subtracted from each spectral line before further processing. In standard mode of operation, at least 150 single power spectra are utilized in this procedure.

Doppler spectra received by MRR is related to the DSD and given by,

$$N(D,z)\Delta D = \frac{\eta(D,z)}{\sigma(D)}\Delta D \tag{1}$$

where $N(D,z)$ is the spectral drop density at a height z and $\eta(D,z)$ is the spectral volume scattering cross section. The single particle back scattering cross section, $\sigma(D)$, of a sphere with diameter, D, is calculated using Mie scattering theory. Under zero vertical wind assumption, terminal fall velocity of a raindrop, v, can be related to the diameter of falling drops by Gunn and Kinzer (1949) as,

$$D(v,z) = \frac{1}{0.6}\ln\frac{10.3}{9.65 - v/\delta(z)} \tag{2}$$

The height dependence of the terminal fall velocity due to change in air density, $\delta(z)$, is approximated as a second-order polynomial (Foote and Du Toit, 1969) given by,

$$\delta(z) = \left(1 + 3.68\times10^{-5}z + 1.71\times10^{-9}z^2\right) \tag{3}$$

Therefore, the spectral volume scattering cross section can be obtained in the Doppler velocity domain as

$$\eta(D,z) = \eta(v,z)\frac{\partial D(v,z)}{\partial v} \tag{4}$$

where $\eta(v,z)$ is directly obtained from the measured Doppler spectrum. Other rain integral parameters, like rain rate, radar reflectivity and liquid water content can be obtained using a standard formulation involving the calculated DSD.

The mean fall Velocity, v_m, is calculated directly from the Spectral power, $p(f)$, related to the Doppler frequency (f) using the first moment as,

$$v_m = \frac{\lambda}{2}\frac{\int_0^\infty f\cdot p(f)df}{\int_0^\infty p(f)df} \tag{5}$$

At 24.1 GHz, rain attenuation is very severe, especially at high rain rate. Gaseous attenuation, on the other hand, can be negligible at this frequency due to small path length in lower troposphere. Therefore, the rain attenuation correction is applied using a recursive algorithm of Kunz (1998). In this technique, all the parameters in the lowest range gate are assumed to have zero rain attenuation. The number density obtained in the lowest range gate is then used to estimate the rain attenuation coefficient (k_r) for the next range gate. The correction term for two way attenuation (A) in next range gate will be,

$$A(z_2) = \exp\left[-2k_r(z_1)\Delta z\right] \tag{6}$$

Range dependent error is another important consideration in radar remote sensing. Sampling uncertainties due to the beam broadening, weakening of signal strength with increase in distance and change in the volume with increase in height are the primary reasons for such error (Berenguer and Zawadzki, 2008, 2009). This kind of error leads to significant underestimation of radar rainfall (Kitchen and Jackson, 1993) in conventional radars measuring the power of received and transmitted signal. In case of MRR, since Doppler principle is used to detect primarily the fall velocity, the effect of range-dependent errors will be less pronounced than the conventional radar. The radar calibration constant of MRR is determined from comparison of MRR observed values with in-situ rain rate measurements in varying environmental conditions by the manufacturer and its uncertainty is said to be within ±10%.

The relation between terminal fall velocity and drop size mentioned in Eq. (2) is the key parameter in MRR retrieval of rain properties. The equation is valid only for stagnant air which is not always a good representation of natural environment. Since the fall velocity is related with vertical wind motion, any non-zero value of the vertical wind will introduce a bias in the retrieved product. The down wind increases the fall velocity of rain drops leads to an artificial overestimation of the drop size as well scattering cross-section which will ultimately cause an underestimation of the drop density. The rain IRPs like rain rate and LWC will also be underestimated in such scenario due to low number of drops. The Doppler retrieval under strong turbulence will, therefore, also be erroneous. A detailed analysis of the errors caused by such assumption is given by Peters et al. (2005). It was, however, noted that the improper vertical wind correction would further deteriorate the quality of estimated parameters in comparison to the original retrieved

data. Therefore, in this study, the zero vertical wind assumption is used.

The MRR can measure the Doppler spectrum with a minimum time resolution of 10 s and 35 m height resolution. However, the radar electronics take almost 6 s for data processing during which no measurements are possible. So to enhance the reliability of data, in this study, MRR time resolution is set to be 30 s. Further, since the first few range gates in 35 m height resolution can be contaminated by ground echo, the height resolution is fixed at 200 m to cover up to 6 km in 30 steps. In tropical regions like Ahmedabad and Trivundrum, the zero degree isotherm is ~4–5 km, so this configuration can essentially able to capture the complete rain region in most of the cases except for a few high convective systems which can go beyond 6 km. For Shillong, the melting layer usually occurs at 3–4 km region above ground since it is a hilly region. With 200 m vertical resolution, finer rain structure may not be adequately captured, but the mean trend can be captured with good accuracy.

2.3. Data pre-processing

The MRR was operated at Ahmedabad during year 2006–2008. For Shillong and Trivandrum, MRR data were obtained for 2007–2008 only. To study the mean vertical profile of the rain, following the methodology of Peters et al. (2005), we first categories the rain in four rain rate region, namely 0.02–0.2 mm/h, 0.2–2 mm/h, 2–20 mm/h and 20–200 mm/h. This methodology is adopted since rain structure is strongly dependent on the rain type, namely convective and stratiform rain. There are numbers of methodologies available to distinguish between stratiform and convective rain. Use of rain rate for classification of rain type is commonly used. Another approach is using the radar bright band signature for identifying stratiform rain (Fabry and Zawadzki, 1995). We use the rain rate ranges for this present study for its simplicity. Previous observations with MRR and Disdrometer at these locations also showed that the ground rain rate can be a good indicator for rain type (Das et al., 2009; Rao et al., 2001).

Since we are mainly interested to study the mean profile of these rain classes, the seasonal variations are also not taken into account. The South-West (SW) and North-East (NE) monsoon may have different rain structure (Kozu et al., 2006), but the difference is primarily originated from the rain type. Further, algorithms usually used in ground-based radars and also in space-borne radars like TRMM to retrieve the rain profile based on rain types and does not consider the seasonal behavior. The seasonal variability and effect of orographic rain on vertical profile will be a subject matter of future investigation and not considered in the present study.

The validity of the MRR data is reported by many researchers from different rain regions (Tokay et al., 2009; Peters et al., 2005; Das et al., 2010a,b, 2011a,b) with satisfactory results. To ensure the robustness of the present study, this data set is further checked on the basis of a few criteria to minimize the instrumental and other unaccounted errors. First, we ascertain that the observed individual profile is complete and no discontinuity is there. This limits the error due to sudden reflection arises due to insect or non-hydrometeors. Secondly, we randomly test the radar data with collocated Disdrometer data to see if there is any discrepancy in the rain pattern. We used rain rate values obtained from the lowest height range (200 m) of the MRR for comparison purpose (Das et al., 2010a,b). One such example is shown in Fig. 2, which indicates a very good matching of ground rain rate and that at 200 m for low rain rate.

The Disdrometer shows a little higher value than MRR for high rain rates as shown in Fig. 2. The underestimation of rain rate in MRR may be due to the considerable rain attenuation at high rain rates for which no attenuation correction is applied at the lowest range gate. This is an important consideration in MRR data processing as at 24.1 GHz rain attenuation is very significant for high rain rate and thus limiting the capability of the instrument. However, this primarily underestimates the derived DSD and other rain parameters, but not severely affects the mean fall velocity of the drops which are calculated directly from the Doppler spectrum. So for high rain rates, the interpretations of the results are supported by the fall velocity spectrum to avoid this pitfall in this study.

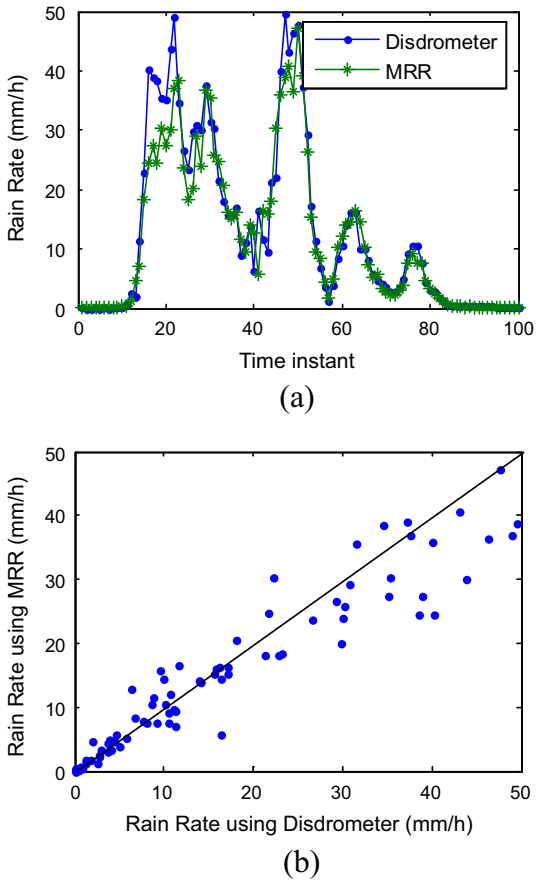

Fig. 2. Rain rate observed during 2020 IST-2120 IST using Disdrometer at ground and MRR at 200 m height at Ahmedabad on 30 August, 2007.

In this study we have also not considered the virga rain type, which may occur in these locations. But since this type of rain does not contribute to the ground rain, we exclude this type of rain from our study. For this purpose, we include in the statistics only the rain profiles which reach to the lowest range gate of MRR nearest to the ground. The number of valid profiles that falls in the specified rain rate range is given in Table 2. In averaging the data set, there are still some possibilities of suppression of information. Peters et al. (2005) showed that this suppression of information is not very serious and the mean dataset can still efficiently serve the purpose of the study.

3. Results

3.1. Stratiform and convective rain

Examples of a stratiform event and a convective event, as observed by MRR at Ahmedabad, are shown in Fig. 3(a) and (b), respectively. The upper subplot shows the reflectivity and lower subplot shows the fall velocity. The ground rain rate for the stratiform type is mostly within 2–5 mm/h whereas in convective case

Table 2
Number of valid profiles at each rain rate range.

Locations/rain rate range	0.02–0.2 mm/h	0.2–2 mm/h	2–20 mm/h	20–200 mm/h
Trivundrum	18,735	21,059	10,112	2023
Ahmedabad	27,585	31,726	17,754	2877
Shillong	20,592	23,841	11,972	2134

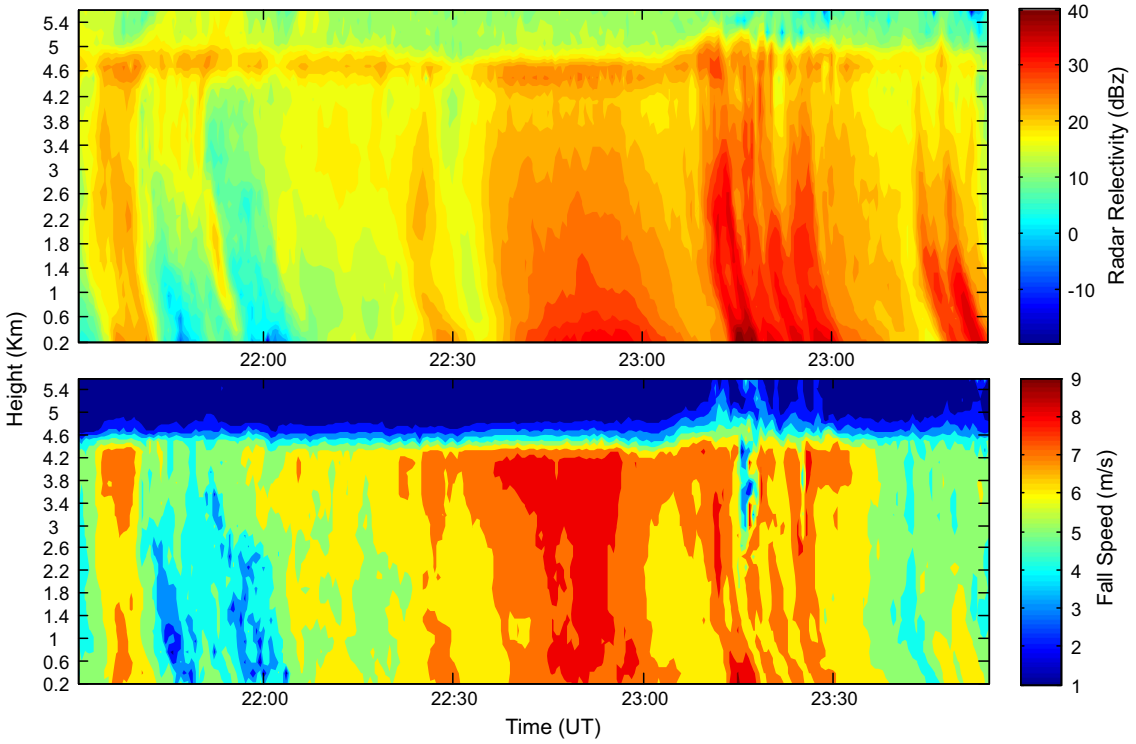

(a)

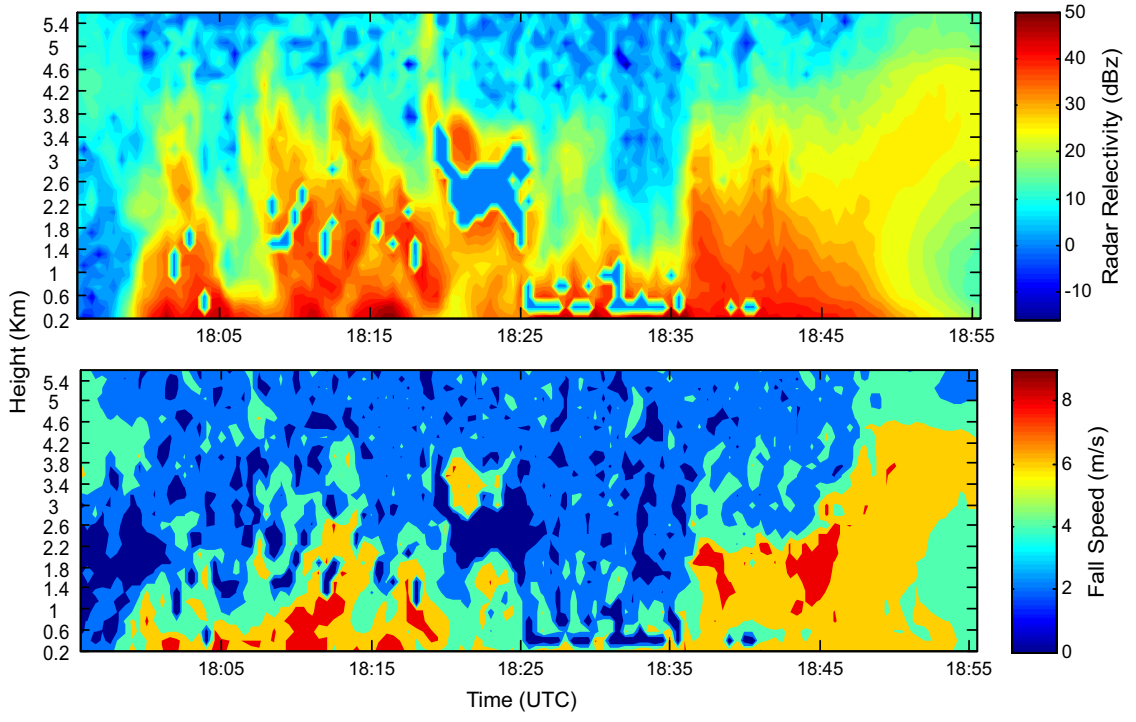

(b)

Fig. 3. (a) Stratiform rain observed by MRR on 3 July, 2006 and (b) convective rain observed by MRR on 3 July, 2006. Upper subplot shows the reflectivity profile and lower subplot shows the fall velocity profile.

the rain rate has a peak value of 25 mm/h with a majority of the rain rates in the range of 8–12 mm/h.

The stratiform rain event shows a clear bright band around 4.6–5 km in reflectivity profile, whereas the fall velocity shows a sharp negative gradient ($dv_m/dz < 0$) around that height. The melting of ice crystals to rain increases the fall velocity. Both fall velocity and radar reflectivity show somewhat uniformity up to the melting layer in stratiform rain. However, we can also note that the radar reflectivity profile is a little bit tilted in the lowest height ranges.

In contrast, the convective rain has no such bright band due to the strong wind motion characterized by the convective activity. The fall velocity and radar reflectivity also show significantly varied vertical profile.

These observations clearly indicate that the radar retrieval will largely be affected by the rain type, especially in the melting layer region. Although this fact is already included in the TRMM rain retrieval algorithms, however, the variation in the lower portion of the spectrum is still ignored.

In order to ascertain the actual characteristics, we, therefore, investigate the mean profile of radar reflectivity and fall velocity. In addition, we also study the mean profile of rain rate and liquid water content to understand the vertical variability of rain. Finally the mean DSD profiles are examined to identify the physical processes which are responsible for such a varied rain structure during the different rain rate regime.

3.2. Mean profile of rain rate, liquid water content, fall velocity and radar reflectivity

To understand the variability of the rain structure under different rain types, we study the profiles of rain rate (R), liquid water content (LWC), fall speed (v_m) and radar reflectivity (Z) for different rain classes as discussed in the following subsections.

3.2.1. Mean profile of radar reflectivity

Mean profile of radar reflectivity for different rain rate classes for different regions are shown in Fig. 4. Melting layer signature in Z-profile is obtained around 5 km in rain rate ranges 0.2–20 mm/h in Ahmedabad and indicates that most of the rain is of stratiform type. However, in 2–20 mm/h rain class, relatively small peak of radar reflectivity at the melting layer height indicates that some of the rain events still have melting layer structure although most of the rain is of convective type. Essentially, this type of 'Mixed rain' occurs during transition period of stratiform and convective rain and in the cases when local convective systems are part of the large stratiform system. However, in the 20–200 mm/h rain class does not show such bright band and essentially represents the convective rain structure. Rain fall in Ahmedabad is mostly occurs during South-West monsoon season (June–September). The ground temperature stay relatively uniform throughout the season and, therefore, no significant variations of melting layer height is expected.

Similar nature of Z-profiles can be seen for Trivandrum and Shillong. However, in case of Trivandrum, the bright band signature is strong between 4.4 and 4.6 km. Shillong, on the other hand, does not have very well defined melting layer structure in the average profile due to the seasonal and diurnal variations of melting layer height (Das et al., 2011a,b) and is distributed in the height ranges between 3 and 4.5 km. The melting layer height is strongly dependent upon the ground temperature. Although, unlike Ahmedabad, Trivandrum encounters rain during both SW and NE monsoon, being located near the equator, has limited seasonal and diurnal variations of ground temperature. On the other hand, Shillong, being a high altitude location, has significant seasonal and diurnal temperature variation, which is responsible for varying

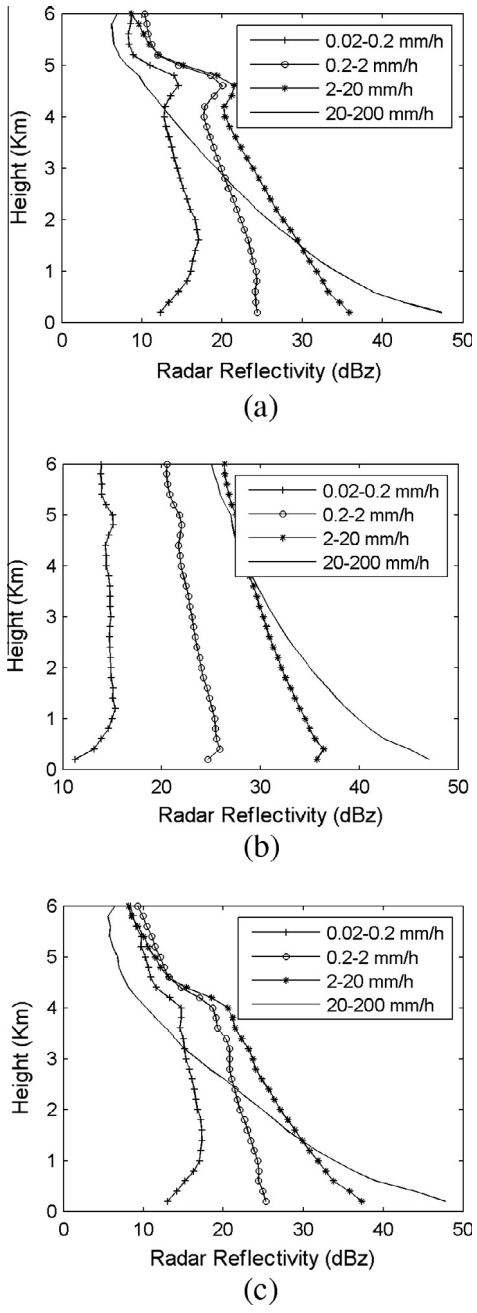

Fig. 4. Average vertical profiles of radar reflectivity at (a) Trivandrum, (b) Ahmedabad and (c) Shillong.

melting layer height. Thus for Shillong, the melting layer signature is distributed as small peaks between 3 and 4.5 km in radar reflectivity profiles.

The radar reflectivity profiles for all the locations mostly show negative slopes with height, but the magnitude of the slopes increase with increasing rain rates However, the Z-profile in lowest rain rate range indicates a positive gradient ($dZ/dz > 0$) up to 1 km height in case of Ahmedabad and Shillong. The positive gradient is extended further up to 1.6 km in case of Trivandrum. Evaporation is the possible reason of such behavior. In very low rain condition, due to evaporation, all the rain drops form aloft can't reach ground, particularly the smaller drops. This phenomena is most prominent in boundary layer region near the ground and hence, the radar reflectivity shows a positive gradient only up to a limited extent. The availability of moisture and temperature actually controls

the evaporation rate and the extent up to which its effect can be seen on radar profiles. The availability of water vapor is maximum in Trivandrum and Shillong due to their climatic conditions. However, throughout the year, temperature at Trivandrum is much higher than Shillong. The evaporation effect is thus maximum at Trivandrum as evident from the Z profile for the 0.02–0.2 mm/h rain rate class.

The convective regime with rain rate above 20 mm/h has the maximum negative gradient of radar reflectivity, although the absolute magnitude varies significantly in different regions. Shillong shows the maximum negative gradient of radar reflectivity whereas Ahmedabad shows the minimum gradient in case of convective rain. Such steep gradients can be due to mixing of ice with water in cloud. Particularly in case of Shillong, being located in the mountainous region, orographic effect can also lead to a mixture of ice with water in convective rain which can induce a steep gradient of Z. Another possibility for such steep gradient is due to inadequate retrieval of radar reflectivity in MRR at rain rate due to large amount of rain attenuation.

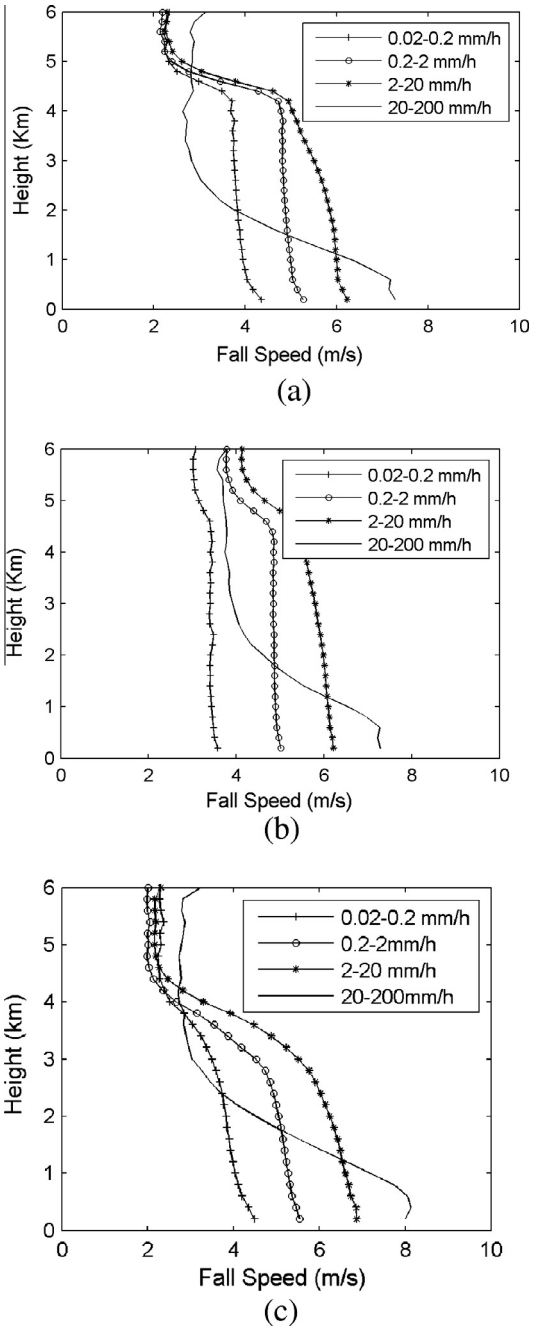

Fig. 5. Average vertical profiles of fall velocity at (a) Trivandrum, (b) Ahmedabad and (c) Shillong.

3.2.2. Mean profile of fall velocity

In contrast to other integral rain parameters (IRP), the mean fall velocity is not susceptible to attenuation or radar calibration. Therefore the mean fall velocities are studied next. Mean fall velocity profiles are also very useful to indicate the melting layer height as shown in Fig. 5. The fall velocity profile show a steep negative gradient above melting layer height in stratiform rain indicate the presence of slow moving ice crystals. We can note that the average melting layer height is very clearly indicated by the fall velocity profile for all these locations.

The fall velocity shows large negative gradient ($dv_m/dz < 0$) just below the melting layer due to conversion of melting ice to water drops. Thus, it gives a good indication of the average rain region where the retrieved IRPs, using the conventional radar retrievals, are valid. We can note that the average rain region for Trivandrum is ~4 km, for Ahmedabad ~4.5 km and for Shillong ~3 km above ground.

The mean fall velocities for all these regions indicate a negative slope ($dv_m/dz < 0$) as well. However, we can also note that the magnitudes of slope of these curves significantly differ among different regions as well as for different rain classes. Rain rate classes 0.02–0.2 mm/h and 0.2–2 mm/h show almost uniform fall velocities of the hydrometeor up to melting layer height for Trivandrum and Ahmedabad. But for Shillong, the negative slope is significant for these two classes also. The observed change in the vertical profiles of fall velocity in Shillong from that of other locations may be due to several reasons. A considerable change in the vertical DSD may occur for the stratiform type of rain in Shillong, which are not observed for Ahmedabad and Trivandrum. Further, varying melting layer height at Shillong can also influence the average fall velocity profiles at the height ranges above 2 km. The convective cases have the highest negative slopes of the fall velocities, which are also supported by the observations from other regions (Thurai et al., 2003; Peters et al., 2005). As already mentioned, a height dependent mixture of ice and water can also leads to strong negative gradient of fall velocity profiles. However, this point cannot be ascertained with the present data set and needs further investigation.

3.2.3. Mean profile of liquid water content

Liquid water content, which is derived based on the DSD, shows some interesting features for these locations as shown in Fig. 6. The lower few km shows a positive gradient (dLWC/dz > 0) for the lowest rain rate range at all the places. However, this positive gradient is still significant for higher rain rate classes in Shillong, negative or slightly positive gradients are observed in other locations at high rain rate ranges. The negative slope is expected as revealed by the radar reflectivity and fall velocity profiles and slight positive gradients can be due to errors introduced by overcompensation of the rain attenuation at high rain rate. The positive gradient in lowest rain rate range, however, cannot be ignored since the possible error due to rain attenuation is very less at this rain rate range. The possible reason for such behavior may be due to the shift of DSD peak toward smaller drops with increasing height. Since the lowest rain rate range usually associated with drizzle, which is closely related to the lower shallow clouds, the fall velocity is less at that height. The fall velocity profile also indicates a negative gradient in velocity at higher altitudes which may be due to smaller drops (Peters et al., 2005; Prat and Barros, 2010). Another factor is that the evaporation, which can be significant

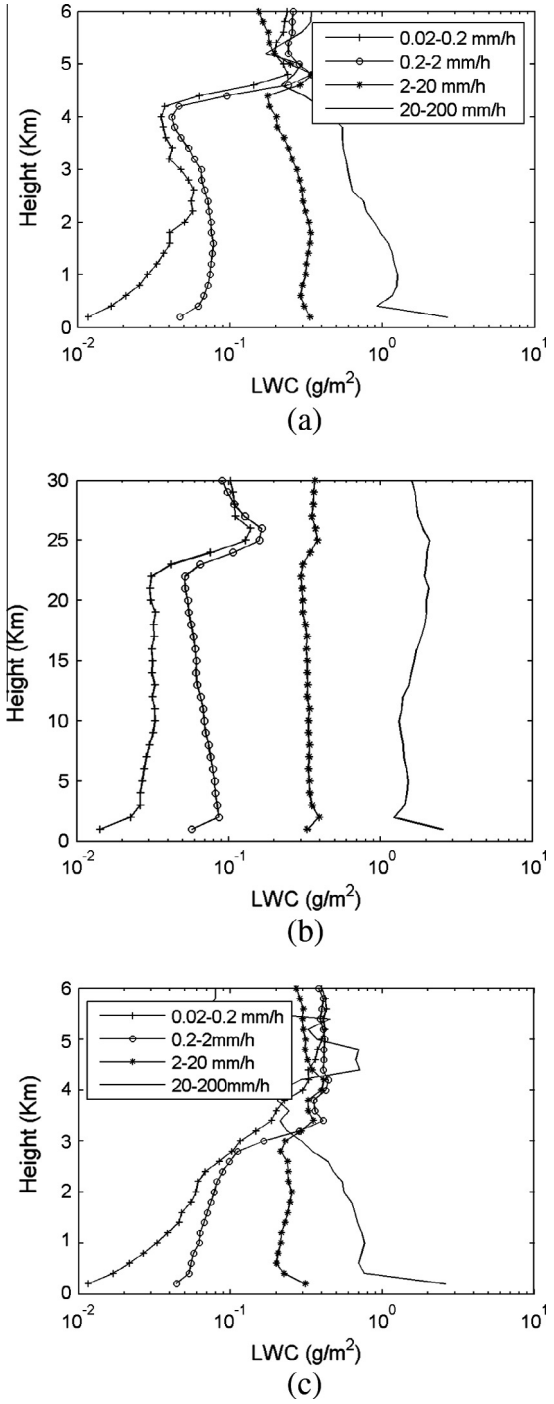

Fig. 6. Average vertical profiles of liquid water content at (a) Trivandrum, (b) Ahmedabad and (c) Shillong.

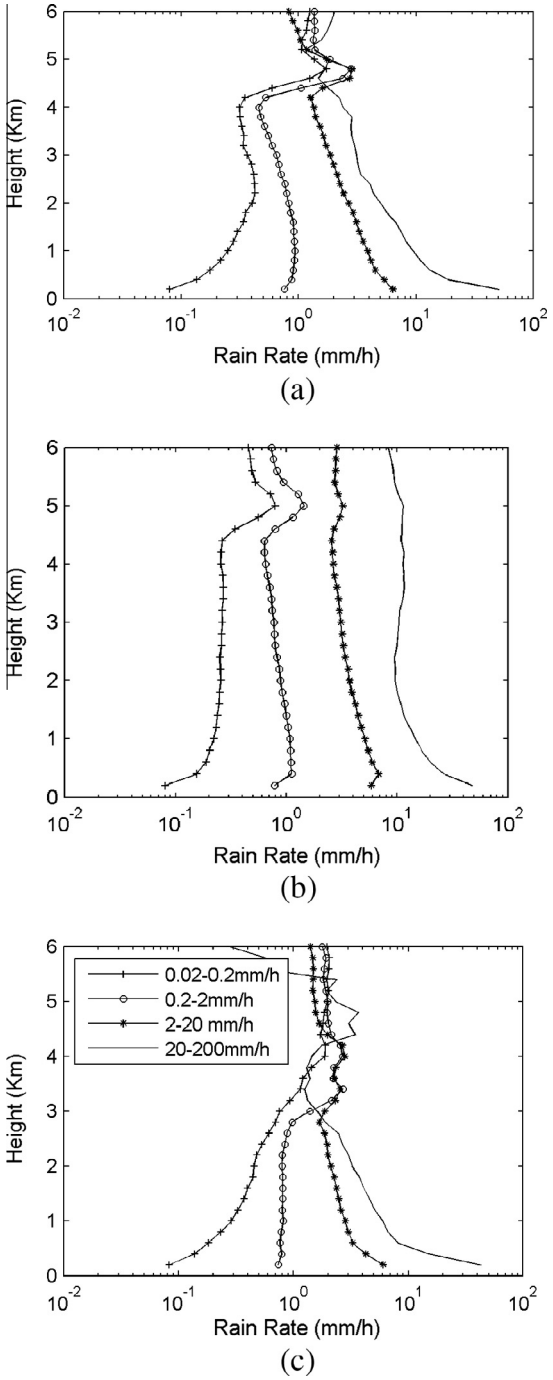

Fig. 7. Average vertical profiles of rain rate at (a) Trivandrum, (b) Ahmedabad and (c) Shillong.

at the very low rain rates and at lower heights, alters the DSD, particularly affecting the small drops concentration. This can also lead to a positive gradient of the LWC profile.

3.2.4. Mean profile of rain rate

The rain rate profile in Fig. 7 indeed show a positive slope in 20–200 mm/h rain class with height above 2 km similar to liquid water profile. This may not be realistic considering the high amount of rain attenuation in this frequency. The positive slope of the rain rate at the lowest rain rate range, however, is not an artefact as already discussed. In general, observations indicate a near uniform or negative trend of the rain rate with height and in accordance with the radar observations from other locations (Thurai et al., 2003; Prat and Barros, 2010; Peters et al., 2005; Tokay et al., 2009).

The rain rate classes 0.2–2 mm/h and 2–20 mm/h show almost uniform behaviors with height for Shillong and a little negative gradient for Ahmedabad, however, Trivandrum shows a significant negative gradient. This indicates that the change in DSD evolution in height are significantly differ among different regions with different climatic conditions. Shillong, being a high altitude location, have difference in drop evolution mechanism with that of Trivandrum, although both have prominent SW and NE monsoon season. This is an important consideration for proper retrieval of rain information from radar observations.

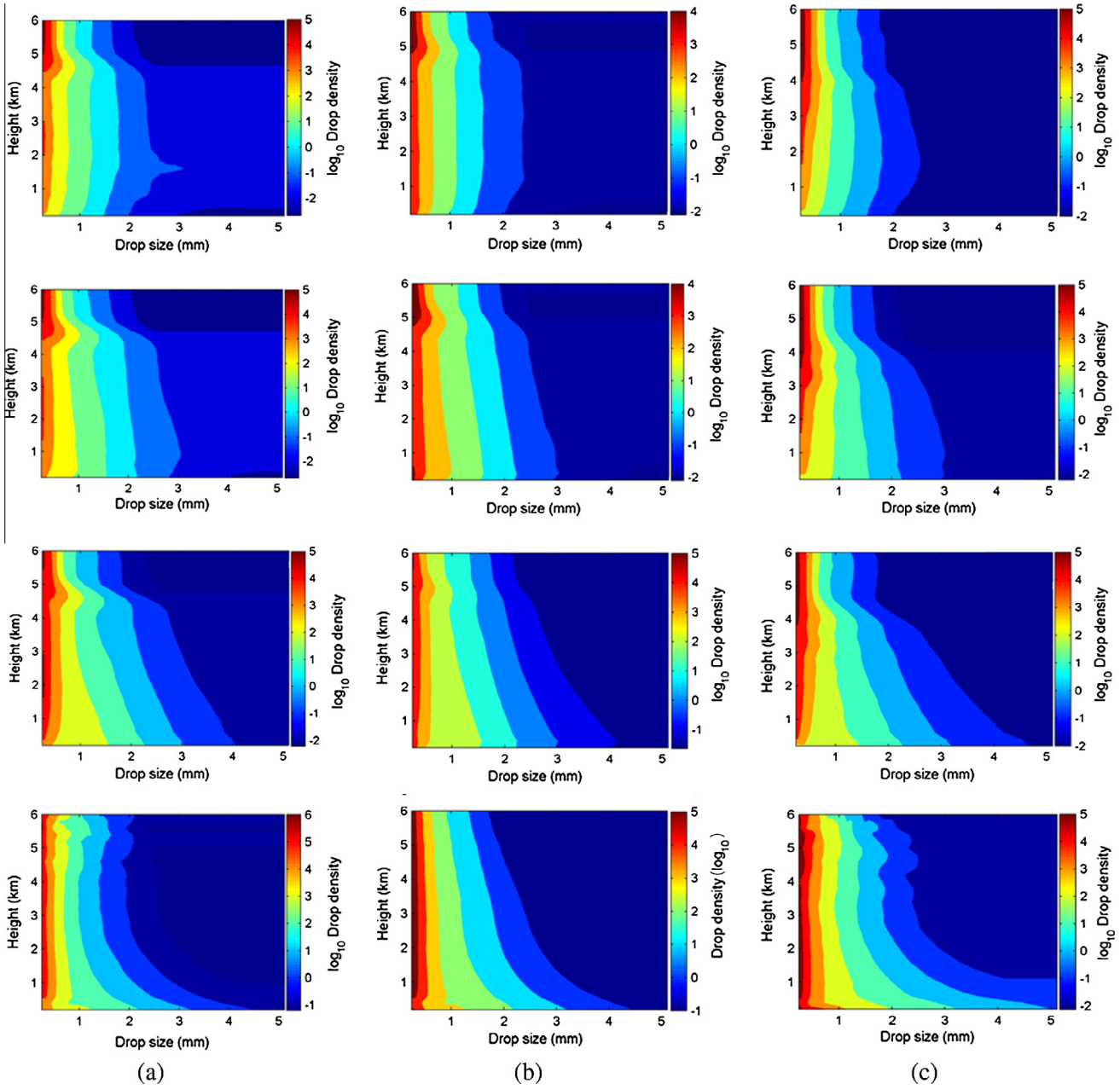

Fig. 8. Average vertical DSD profiles at (a) Trivandrum, (b) Ahmedabad and (c) Shillong. Different DSD figures in each panel corresponds to the rain rates ranges as indicated in previous figures. The top most figures correspond to the lowest rain rate range (0.02–0.2 mm/h) and bottom most figures indicate the highest rain rate range (20–200 mm/h).

3.3. Mean drop size distribution and drop evolution mechanism

Drop size distribution holds the key to understand the characteristic difference observed in different regions and important to characterize the tropical rain. Ground based DSD measurements are reported by many researchers (Kozu et al., 2006; Rao et al., 2009; Das et al., 2010a,b) indicating the change due to stratiform and convective rain. However, this is the first such attempt from the Indian region to study the growth and evolution of vertical DSD structure in relation with the mean VPR.

The mean drop size of these rain classes measured at different locations are shown in Fig. 8. One should note that the DSD profiles are valid only in the rain region, i.e., below the melting layer height and our discussion is limited to that region only.

The lowest rain class shows a significant decrease in bigger drops with decreasing height ($dD/dZ > 0$) at near ground region (boundary layer region) and can indicate the occurrence of drop break-up mechanism. The total number of small drops is also reduced with decreasing height. This effect is more prominent in case of Trivandrum and Shillong. As already pointed out, the evaporation of smaller drops could be the possible reason for such. Above the boundary layer region and up to melting layer height, the DSD is almost uniform for Ahmedabad. This indicate that the drop break up, coalescence and evaporation are just in balance to maintain the DSD throughout the height. However, a negative slope ($dD/dz < 0$) for the drops of large size and a positive slope of small drop concentration ($dN/dz > 0$) can be noticed in case of Shillong and Trivandrum, which is particularly significant for Shillong. Sufficient availability of moisture in both these cases may be responsible for counter balance the evaporation effect at these heights and favor the drop coalecence. In case of Shillong, in addition to the moisture availability, the orographic enhancement can

lead to strong upward wind motion, which will further favor the drop coalescence process. Thus we get more number of large drops at lower heights at the expense of large number of smaller drops at higher heights in case of Shillong.

For the 0.2–2 mm/h rain class, the vertical profiles for all the locations indicate dominance of drop coalescence process as more large drops are more abundant just above the boundary layer than at higher heights. The concentration of very small drops also decreases with decrease in heights ($dN/dz > 0$) above boundary layer region. However, in boundary layer region the drop break up dominates. In boundary layer region, the decrease in small drop number ($dN/dz > 0$) without any significant increase in large drop ($dD/dz < 0$) still indicate role of evaporation. We can actually note that a small but noticeable increase in drop concentration (dN/dz) of medium drop sizes in terms of broadening of drop concentration peak in the lower side of the DSD.

For the 2–20 mm/h rain class, more changes of DSD are observed. Evaporation is no longer a factor for any of these locations. The largest drop size shows strong negative gradient ($dD/dz < 0$). For Trivandrum and Ahmedabad, the largest drop size reaches up to 4 mm at ground level whereas it can go up to 4.5 mm in case of Shillong. However, the drop size gradient is smaller in Ahmedabad compared to that in Shillong. The large gradient is due to drop coalescence process which further indicate a strong convective or orographic enhancement in Shillong. Smaller drop concentration, although, shows a positive gradient ($dN/dz > 0$), however, the DSD peak has become wider at 0.5–1.4 mm range at the ground. Drop coalescence seems to be stronger mechanism in Shillong, than for Ahmedabad and Trivandrum. This result indicate that since this rain rate class represent both stratiform and convective rain, both the drop evolution mechanisms, namely coalescence and break up, are effective.

The convective rains in the 20–200 mm/h rain class show completely different rain drop evolution mechanism responsible for different regions. Trivandrum and Shillong are characterized by a uniform DSD variation at higher heights and drop coalescence seems to be strong in lower heights. But for Ahmedabad, the drop coalescence is the dominant mechanism throughout the height ranges. The large drop up to 5 mm has a significant concentration at near ground level in case of Shillong, which is not observed for other two places. It is to be noted that the interpretation of the vertical profiles in 20–200 mm/h rain rate range is rather complex due to significant rain attenuation at these rain rates. We also have implicitly assumed that the profiles correspond this rain rate range is due to water drop. However, mixture of ice and water is a possibility in convective conditions as well due to orographic enhancement, as already mentioned. This may lead to inadequate interpretation of the drop evolution mechanism. A better characterization of this kind of rain is therefore needed further investigation in a comprehensive manner, particularly with dual polarization observations to separate the ice from water.

4. Conclusions

Vertical structure of reflectivity and drop size distributions are important considerations for accurate estimation of rain information from radar observation. The vertical evolution of DSD is also important to study and characterize the rain. The vertical structure of rain measured using MRR at three locations reveal some features of tropical rain which may have important consequences in space based radar retrieval of precipitation. The results support the fact that the vertical profile of reflectivity has a very sharp gradient due to melting layer. However a strong variation of VPR is also observed in high rain rates above 20 mm/h for all the locations. This variation exists at even low rain rate in Shillong, a high altitude location. The DSD is found to be responsible for such in VPR. The VPR and retrieved rain parameters indicate a significant change of DSD during various rain rate regimes and for different locations. Consequently, the drop evolution mechanism throughout the height range is studied by MRR and it is found, in general, that the drop break-up mechanism is dominant in stratiform rain and drop coalescence in convective rain. Convective rain is found to have larger drop size at ground level than that of stratiform rain. Further, different locations also show dominance of different drop evolution mechanism at different height ranges. The study highlights the characteristic difference of varied rain type and effects of local climatic conditions in controlling the rain structure.

Acknowledgments

Authors thankfully acknowledge the financial support received under Indian Space Research Organisation (ISRO) sponsored Space Science Promotion Scheme. Authors also thanks the scientist of Space Applications Centre, ISRO for their effort in establishing the radars and collecting the data.

References

Atlas, D., Srivastava, R., Sekhon, R., 1973. Doppler radar characteristics of precipitation at vertical incidence. Rev. Geophys. Space Phys. 11, 1–35.

Bellon, A., Lee, G.W., Zawadzki, I., 2005. Error statistics of VPR corrections in stratiform precipitation. J. Appl. Meteorol. 44, 998–1015. http://dx.doi.org/10.1175/JAM2253.1.

Bellon, A., Lee, G.W., Kilambi, A., Zawadzki, I., 2007. Real-time comparisons of VPR-corrected daily rainfall estimates with a gauge mesonet. J. Appl. Meteorol. Climatol. 46, 726–741. http://dx.doi.org/10.1175/JAM2502.1.

Berenguer, M., Zawadzki, I., 2008. A study of the error covariance matrix of radar rainfall estimates in stratiform rain. Weather Forecast. 23, 1085–1101.

Berenguer, M., Zawadzki, I., 2009. A study of the error covariance matrix of radar rainfall estimates in stratiform rain. Part II: scale dependence. Weather Forecast. 24, 800–811.

Cluckie, I.D., Griffith, R.J., Lane, A., Tilford, K.A., 2000. Radar hydrometeorology using a vertically pointing radar. Hydrol. Earth Syst. Sci. 4, 565–580. http://dx.doi.org/10.5194/hess-4-565-2000.

Das, S., Shukla, A.K., Maitra, A., 2009, Classification of convective and stratiform types of rain and their characteristics features at a tropical location. In: 4th International Conference on Computers and Devices for Communication, Kolkata, India, Dec. 14–16, 2009.

Das, S., Maitra, A., Shukla, A.K., 2010a. Rain attenuation modeling in the 10–100 GHz frequency using drop size distributions for different climatic zones in tropical India. Progr. Electromagn. Res. B 25, 211–224.

Das, S., Shukla, A.K., Maitra, A., 2010b. Investigation of vertical profile of rain microstructure at Ahmedabad in Indian tropical region. Adv. Space Res. 45 (10), 1235–1243. http://dx.doi.org/10.1016/j.asr.2010.01.001.

Das, S., Talukdar, S., Bhattacharya, A., Adhikari, A., and Maitra, A., 2011. Vertical profile of Z-R relationship and its seasonal variation at a tropical location. In: Applied Electromagnetics Conference (AEMC), Kolkata, India, Dec. 18–22, 2011. http://dx.doi.org/10.1109/AEMC.2011.6256915.

Das, S., Maitra, A., Shukla, A.K., 2011b. Melting layer characteristics at different climatic conditions in the Indian region: ground based measurements and satellite observations. Atmos. Res. 101 (1), 78–83.

Fabry, F., Zawadzki, I., 1995. Long-term radar observations of the melting layer of precipitation and their interpretation. J. Atmos. Sci. 52, 838–851.

Foote, G.B., Du Toit, P.S., 1969. Terminal velocity of raindrops aloft. J. Appl. Meteorol. 8 (249), 253.

Gunn, R., Kinzer, G.D., 1949. The terminal velocity of fall for water droplets in stagnant air. J. Meteorol. 6, 243–248.

Kitchen, M., Jackson, P.M., 1993. Weather radar performance at long range: simulated and observed. J. Appl. Meteorol. 32, 975–985.

Kirstetter, P.E., Andrieu, H., Boudevillain, B., Delrieu, G., 2013. A physically based identification of vertical profiles of reflectivity from volume scan radar data. J. Appl. Meteorol. Climatol. 52, 1645–1663. http://dx.doi.org/10.1175/JAMC-D-12-0228.1.

Koistinen, J., Michelson, D.B., 2002. BALTEX weather radar-based precipitation products and their accuracies. Boreal Environ. Res. 7, 253–263.

Kozu, T., Reddy, K.K., Mori, S., Thurai, M., Ong, J.T., Rao, D.N., Shimomai, T., 2006. Seasonal and diurnal variations of raindrop size distribution in Asian monsoon region. J. Meteorol. Soc. Jpn. 84A, 195–209.

Kunz, M., 1998. Niederschlagsmessungen mit einem vertikal ausgerichteten K-Band FM-CW-Dopplerradar. Diplomarbeit (Diploma thesis), Institut für Meteorologie und Klimaforschung, Universität Karlsruhe. 95p.

Peel, M.C., Finlayson, B.L., McMahon, T.A., 2007. Updated world map of the Köppen–Geiger climate classification. Hydrol. Earth Syst. Sci. 11, 1633–1644. http://dx.doi.org/10.5194/hess-11-1633-2007.

Peters, G., Fischer, B., Münster, H., Clemens, M., Wagner, A., 2005. Profiles of raindrop size distributions as retrieved by microrain radars. J. Appl. Meteorol. 44, 1930–1949. http://dx.doi.org/10.1175/JAM2316.1.

Prat, O.P., Barros, A.P., 2010. Ground observations to characterize the spatial gradients and vertical structure of orographic precipitation – experiments in the inner region of the Great Smoky Mountains. J. Hydrol. 391 (1–2), 141–156. http://dx.doi.org/10.1016/j.jhydrol.2010.07.013.

Rao, T.N., Rao, D.N., Mohan, K., Raghavan, S., 2001. Classification of tropical precipitating systems and associated Z-R relationships. J. Geophys. Res. 106 (D16), 17699–17711. http://dx.doi.org/10.1029/2000JD900836.

Rao, T.N., Radhakrishna, B., Nakamura, K., Rao, N.P., 2009. Differences in raindrop size distribution from southwest monsoon to northeast monsoon at Gadanki. Q. J. R. Meteorol. Soc. 135 (643), 1630–1637.

Rudolph, J.V., Friedrich, K., 2013. Seasonality of vertical structure in radar-observed precipitation over Southern Switzerland. J. Hydrometeorol. 14, 318–330. http://dx.doi.org/10.1175/JHM-D-12-042.1.

Seo, D.J., Breidenbach, J., Fulton, R., Miller, D., O'Bannon, T., 2000. Real-time adjustment of range-dependent biases in wsr-88d rainfall estimates due to nonuniform vertical profile of reflectivity. J. Hydrometeorol. 1, 222–240. http://dx.doi.org/10.1175/1525-7541(2000) 001<0222:RTAORD>2.0.CO;2.

Thurai, M., Iguchi, T., Kozu, T., Eastment, J.D., Wilson, C.L., Ong, J.T., 2003. Radar observations in Singapore and their implications for the TRMM precipitation radar retrieval algorithms. Radio Sci. 38, 1086. http://dx.doi.org/10.1029/2002RS002855.

Tokay, A., Hartmann, P., Battaglia, A., Gage, K.S., Clark, W.L., Williams, C.R., 2009. A field study of reflectivity and Z-R relations using vertically pointing radars and disdrometers. J. Atmos. Oceanic Technol. 26, 1120–1134. http://dx.doi.org/10.1175/2008JTECHA1163.1.

Zipser, E.J., Lutz, K.R., 1994. The vertical profile of radar reflectivity of convective cells: a strong indicator of storm intensity and lightning probability? Mon. Weather Rev. 122, 1751–1759.